J. of Thermal Science Vol.2, No.2

Journal of Thermal Science
Science Press 1993

Mathematical Simulation of Evaporating Brine by Solar Radiation for the Production of Salt

Y.Z. **Zhang** **X.S.** *Ge* **Y.F. Li**

Dept. of Engineering Thermophysics, University of Science and Technology of China, Hefei, Anhui 230026, China

C.D. Li

Scientific and Technological Division, Jiangsu Provincial Salt Cooperation, Lianyungang, Jiangsu, China

A computer simulation model of salt pan is presented. The transient behavior and the effects of various parameters of the salt pans, such as the depth of the brine layer, the absorptance of the soil surface, the thermal properties of the soil beneath the brine layer and the depth of the underground water table, on the evaporation process of salt pans are discussed. The effects of extra insulation layer and the intensity of solar radiation are also examined.

Keywords: salt pan, solar radiation, simulation.

INTRODUCTION

Evaporating brine in the sun has long been the most fundamental method to make salt. In China there are many coastal salt pans producing salt for edibility and industry use. Although the solar pond has attracted the attention of many investigators and engineers for its capability of collecting solar energy in large scale at cheap costs and for its long term thermal storage capacity[1–8], little attention, if any, has been paid to date to intensify the process of evaporating brine by solar radiation to make salt.

The objective of this paper is to study the evaporation rate of brine of the shallow salt pans and its relation to various parameters in the process of evaporating sea water. With a developed simulation model combined with the meteorological conditions, the transient behavior and the effects of various parameters of the salt pans such as the depth of the brine layer, the absorptance of the soil surface, the thermal properties of the soil beneath the brine layer and the depth of the underground water table, on the evaporation process of salt pans are discussed. The effects of extra insulation layer and the intensity of solar radiation are also computed and examined.

Received June, 1993.

SIMULATION MODEL

Generally, the process of evaporating brine in the sun to obtain edible salt is a process of evaporating the brine in many separated shallow salt pans which are connected in series. That is, the brine with low salt concentration (natural sea water) evaporates in a salt pan for several days and then flows into the next salt pan with a higher salt concentration, and the process of evaporation continues; thus the salt concentration of the brine increases step by step. When the salt concentration reaches a certain value, the brine is collected into a storage pond, or in some cases, pumped into a heated pan, to let the salt separate. The whole process from evaporating sea water to the crystallization of salt usually takes 3–4 weeks.

Although the evaporating process in the salt pan is a little bit similiar to that of solar still technology, the salt pan is more closely related to the solar pond. However, the salt pan is much shallower than the solar pond (the depth of the brine layer is about 0.02 to 0.5 M depending on the localities), and thus the response of the salt pans to meteorological conditions such as intensity of solar radiation, ambient temperature, ambient wind speed and ambient relative humidity, is much faster, and these make the evaporation process of the salt pan quite peculiar.

Nomenclature

α	thermal diffusivity of air
α_w	thermal diffusivity of brine
A_s	surface area of a unit of salt pan
α_b	absorptance of soil surface
α_{wbi}	absorptance of brine for beam radiation in the ith wavelength interval
α_{wdi}	absorptance of brine for diffuse radiation in the ith wavelength interval
β	volumetric thermal expansion coefficient
C_w	specific heat of brine
C_{soil}	specific heat of soil
D_{AB}	mass diffusion coefficient
D_w	thickness of brine layer
ϵ_w	emissivity of brine water
g	gravitational acceleration
h_{fg}	latent heat of vaporization
h_m	convection mass trnasfer coefficient
I_b	intensity of solar beam radiation
I_d	intensity of solar diffuse radiation
k_{bi}	extinction coefficient of brine for beam radiation in the ith wavelength interval
k_{di}	extinction coefficient of brine for diffuse radiation in the ith wavelength interval
k	thermal conductivity of ambient air
k_{soil}	thermal conductivity of soil
L	characteristic length
M_w	mass of brine in a unit area
Nu	Nusselt number
ρ_w	mass density of brine
ρ_{soil}	mass density of soil
$\rho_{a,s}$	mass density of steam in the ambient air at its saturation temperature T_a
$\rho_{w,s}$	mass density of brine vapor at saturation temperature
p_B	fraction of the incident beam solar radiation transmitted into the brine
p_D	fraction of the incident diffuse solar radiation transmitted into the brine
p	perimeter of a unit of salt pan
Ra_L	Rayleigh number
Re	Reynolds number
Sc	Schmidt number
Sh	Sherwood number
T_a	ambient temperature
T_w	temperature of brine
U_o	wind velocity
ν	kinematic viscosity of air
ν_w	kinematic viscosity of brine
ϕ	latitude of salt pan
ϕ_a	relative humidity of ambient air
ω	solar time anger
σ	Stefan–Boltzmann constant
Δx_i	depth of ith divided layer

Subscript

a	ambient air
b	beam radiation
c	convection
d	diffuse radiation
E	evaporation
i	the ith wavelength interval
r	radiation
w	brine water

A schematic cross section of the salt pan is shown in Fig.1. For convenience and without loss of reality and generality, the following simulation syustem to be analyzed is assumed one dimensional, and is divided into two parts: the brine layer and the ground.

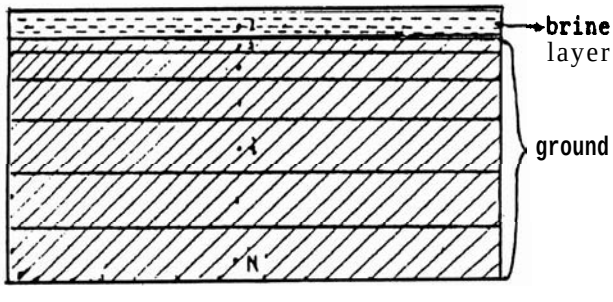

Fig.1 Physical model of the simulation system

Brine Layer

Since the convective heat transfer is much greater than heat conduction and the depth of brine layer is rather thin, the temperature difference inside the brine layer is very small, and it is reasonable to assume that the temperature and salinity in the brine layer is uniform and the lumped heat capacity analysis can be applied. The thermal balance equation for the brine layer of a unit area is:

$$Q_{sun,w} + Q_{c,s-w} = Q_{c,w-a} + Q_{r,w-a} + Q_E + M_w C_w \frac{dT_w}{d\tau} \quad (1)$$

(Rate of solar energy absorbed by the brine + rate of heat transferred from the bottom of the salt pan to the brine by convection = rate of heat loss from the brine to the ambient air by convection + rate of heat loss from the brine to the sky by radiation + rate of heat for the use of evaporation of brine + rate of energy stored in the brine)

The thermal performance of salt pan largely depends on the amount of solar radiation absorbed by

the brine. Although the solar radiation in the long wave range is absorbed by the brine within minimeters, its short wave radiation penetrates the brine layer very deep and, therefore, a proper evaluation of the absorption of solar radiation in the brine is very important for studying the thermal behavior and efficiency of salt pan. Taking account of the multiple reflection processes between the bottom and the free surface of the brine layer, the solar energy absorbed by the brine is expressed as follows:

$$Q_{sun,w} = \sum_i I_{bi} p_B \alpha_{wbi} [1 + (1 - \alpha_{wbi})(1 - \alpha_b)] \times \left(\frac{1}{1 - (1 - \alpha_{wbi})^2 (1 - \alpha_b)(1 - p_B)} \right) + \sum_i I_{di} p_D \alpha_{wdi} [1 + (1 - \alpha_{wdi})(1 - \alpha_b)] \times \left(\frac{1}{1 - (1 - \alpha_{wdi})^2 (1 - \alpha_b)(1 - p_D)} \right) \quad (2)$$

where

$$I_{bi} = \eta_{bi} I_b \qquad I_{di} = \eta_{di} I_d \quad (3)$$

$$\alpha_{wbi} = 1 - e^{-k_{bi} D} \qquad \alpha_{wdi} = 1 - e^{-k_{di} D} \quad (4)$$

In the above expressions, I_b and I_d respectively refer to solar beam and diffuse radiation; a, and α_b are the absorptance of the brine and the soil surface respectively; p_B and p_D are the fraction of the incident beam and diffuse solar radiation transmitted into the brine respectively; k is the extinction coefficient of brine; subscripts b and d denote the beam and diffuse radiation, subscript i denotes the ith wavelength interval; η_{bi} and η_{di} are the fraction of the total solar beam and diffuse radiation involved in the ith wavelength interval. η_{bi}, η_{di} and k_{bi}, k_{di} with different concentrations are adopted from K. Kanayama and H. Bada[9]. D is the optical path length for sunlight travel in the brine layer and is related to the thickness of the brine layer D_w by

$$D = D_w / \cos\gamma \quad (5)$$

where γ is the angle of refraction (the angle between the light beam and the vertical direction). Also we have:

$$\sin i / \sin\gamma = n_1 \quad (6)$$

where n_1 is the refraction index for brine[10]. The incidence angle i is related to the local latitude, the solar declination angle and the appropriate hour of the day as follows[11]:

$$\cos i = \sin\delta \sin\phi + \cos\delta \cos\phi \cos\omega \quad (7)$$

The declination angle δ is a function of the day of the year n[11]:

$$\delta = 23.45 \sin\left(2\pi \frac{284 + n}{365}\right) \quad (8)$$

The reflective loss of the incident solar radiation at the brine surface of the salt pan is also very complicated and difficult to calculate. For a smooth water surface, the ratio of the beam radiation penetrated through the surface to that incident on the surface can be obtained by using Fresnel's law[12]:

$$p_B = 1 - 0.5\left[\frac{\sin^2(i-\gamma)}{\sin^2(i+\gamma)} + \frac{\tan^2(i-\gamma)}{\tan^2(i+\gamma)}\right] \quad (9)$$

For diffuse radiation, a conservative value of 0.9 is assumed for p_d for the present study.

Assuming combined laminar and turbulent air flow over the surface, the convective heat loss from the brine layer to the ambient air is given by [13]:

$$Q_{c,w-a} = h_{c,w-a}(T_w - T_a) \quad (10)$$

$$h_{c,w-a} = \frac{k}{L} Nu = \frac{k}{L}(0.037 Re^{0.8} - 871) Pr^{1/3} \quad (11)$$

$$Re = \frac{U_o L}{\nu} \qquad L = \frac{A_s}{P} \quad (12)$$

where U_o is the wind velocity; k is the thermal conductivity of air; ν is the kinematic viscosity of air; L is the characteristic length; A, and P are the surface area and perimeter of a unit of salt pan.

The Reynolds analogy of heat and mass transfer is used to determine the rate of energy for the use of evaporation[13], that is:

$$Sh = (0.037 Re^{0.8} - 871) Sc^{1/3} \quad (13)$$

$$Q_E = h_{fg} h_m [\rho_{w,s} - \phi_a \rho_{a,s}(T)] \quad (14)$$

$$h_m = \frac{Sh_L D_{AB}}{L} \quad (15)$$

where h_{fg} is the latent heat of vaporization; h_m is the convection mass transfer coefficient; $\rho_{w,s}$ the mass density of brine vapor at saturation temperature; ϕ_a the relative humidity of the ambient air; $\rho_{a,s}$ the mass density of vapor in the ambient air at its saturation temperature T_a; D_{AB} the mass diffusion coefficient.

When there is no wind, the convective heat transfer from the brine layer to ambient air is expressed as follows[13]:

$$Nu_L = 0.54 Ra_L^{1/4} \quad (10^5 \le Ra_L \le 10^7) \quad (16)$$

$$Nu_L = 0.15 Ra_L^{1/3} \quad (10^7 \le Ra_L \le 10^{10}) \quad (17)$$

$$Ra_L = \frac{g\beta_a(T_w - T_a)L^3}{\nu\alpha} \tag{18}$$

where g is the gravitational acceleration; β the volumetric thermal expansion coefficient; a the thermal diffusivity of air. The heat and mass transfer analogy is also used to determine the free convection mass transfer, that is:

$$Sh_L = \frac{Nu_L}{Pr^{1/4}}Sc^{1/4} \quad (10^5 \le Ra_L \le 10^7) \tag{19}$$

$$Sh_L = \frac{Nu_L}{Pr^{1/3}}Sc^{1/3} \quad (10^7 \le Ra_L \le 10^{10}) \tag{20}$$

The free convection heat transfer coefficient between soil surface and brine is pointed out by Globe et al[14] as:

$$h_{c,s-w} = \frac{k}{D_w}Nu = \frac{k}{D_w}0.069Ra^{1/3}Pr^{0.074} \quad 10^5 < Ra_L < 7\times 10^9) \tag{21}$$

where

$$Ra = \frac{g\beta D_w^3(T_{soil} - T_w)}{\nu_w\alpha_w} \tag{22}$$

then

$$Q_{c,s-w} = h_{c,s-w}(T_{soil} - T_w) \tag{23}$$

The radiation loss from brine to the sky can be expressed as follows:

$$Q_{R,w-a} = \varepsilon_w\sigma(T_w^4 - T_{sky}^4) = h_{r,w-a}(T_w - T_{sky}) \tag{24}$$

where

$$h_{r,w-a} = \varepsilon\sigma(T_w^2 + T_{sky}^2)(T_w + T_{sky}) \tag{25}$$

and ε_w is the emissivity of the brine water; a the Stefan–Boltzmann constant; the sky temperature T_{sky} is suggested by Liu et al[15] as:

$$T_{sky} = \left[0.9T_w^4 - (0.32 - 0.026e_d^{0.5}) \times (0.30 + 0.70S)T_a^4\right]^{1/4} \tag{26}$$

where e_d is the vapor pressure in ambient air in mbars, and S is the ratio of the actual insolation hours to that of possible sunshine, it is closely related to the cloudiness.

Ground

The heat loss to the ground requires the evaluation of the temperature profile in the ground. The governing equation for one–dimensional transient heat conduction is

$$\frac{\partial}{\partial x}\left(k_{soil}\frac{\partial T}{\partial x}\right) = \rho_{soil}C_{soil}\frac{\partial T}{\partial \tau} \tag{27}$$

where the coordinate x is positive in the downward direction and measured from the top surface of the soil; $k_{soil}, \rho_{soil}, C_{soil}$ are the thermal conductivity, mass density and specific heat of the soil respectively, and it is assumed that these properties are constant in the temperature range discussed.

At a finite depth D_{wT} below the ground surface, there is a water table with a constant temperature that equals the annual average ambient temperature T_a, that is:

$$T = \overline{T}_a \quad \text{at} \quad x = D_{wT} \tag{28}$$

For the top surface of the soil, the heat balance equation is:

$$-k_{soil}\frac{\partial T}{\partial x}\Big|_{x=0} = Q_{sun,s} - Q_{c,s-w} \tag{29}$$

where $Q_{sun,s}$ is the solar radiation absorbed by the soil surface and is expressed as:

$$Q_{sun,s} = \sum_i I_{bi}p_B(1-\alpha_{wbi})\alpha_b \times\left(\frac{1}{1-(1-\alpha_{wbi})^2(1-\alpha_b)(1-p_B)}\right) + \sum_i I_{di}p_D(1-\alpha_{wdi})\alpha_b \times\left(\frac{1}{1-(1-\alpha_{wdi})^2(1-\alpha_b)(1-p_D)}\right) \tag{30}$$

SIMULATION PROCEDURES

To make the simulation, the soil are divided into n layers. The thickness of each layer increases with the depth, with thermal properties uniform and the node is located in the midst of each layer.' Following the numerical process suggested by Patankar[16], the energy conservation for each layer can be updated from the previous time step by:

$$a_i^{J+1}T_i^{J+1} = a_{i+1}^J T_{i+1}^J + a_{i-1}^J T_{i-1}^J + a_i^J T_i^J \tag{31}$$

where the terms with superscripts J and J + 1 are terms at the time J and J + 1. The subscripts i and $i+1, i-1$ denote the ith node and its two neighboring nodes.

For the brine layer (node 1), the discrete equation is:

$$T_1^{J+1} = a_1^J T_1^J + a_2^J T_2^J + C_1(Q_{sun,w}^J - Q_E^J) + a_a^J T_a^J \tag{32}$$

where

$$a_1^J = 1 - C_1(h_{c,s-w}^J + h_{c,w-a}^J + h_{r,w-a}^J \quad (33)$$

$$a_2^J = C_1 h_{c,s-w}^J \quad (34)$$

$$a_a^J = C_1(h_{c,w-a}^J + h_{r,w-a}^J) \quad (35)$$

$$C_1 = \frac{\Delta\tau}{\rho_w C_w \Delta x_1} \quad (36)$$

T_1 and T_2 are the temperature of brine and the temperature of soil surface respectively; and $A\tau$ is the time step.

For the soil surface (node 2), the discrete equation is:

$$T_2^{J+1} = b_2^J T_2^J + b_1^J T_1^J + b_3^J T_3^J + C_2 Q_{sun,s}^J \quad (37)$$

where

$$b_1^J = C_2 h_{c,s-w}^J \quad (38)$$

$$b_2^J = 1 - C_2\left(h_{c,s-w}^J + \frac{2k_{soil}}{\Delta x_2 + \Delta x_3}\right) \quad (39)$$

$$b_3^J = C_2 \frac{2k_{soil}}{\Delta x_2 + \Delta x_3} \quad (40)$$

$$C_2 = \frac{A\tau}{\rho_{soil} C_{soil} \Delta x_2} \quad (41)$$

For the ground layer (node 3 to node N + 1), the discrete equation is expressed as:

$$a_i T_i^{J+1} = a_{i+1}^J T_{i+1}^J + a_{i-1}^J T_{i-1}^J + a_i^J T_i^J \quad (42)$$

where

$$a_i^J = \frac{\rho C \Delta x_i}{\Delta\tau};$$

$$a_{i-1}^J = \frac{2k_{soil}}{\Delta x_i + \Delta x_{i-1}} \quad (43)$$

$$a_{i+1}^J = \frac{2k_{soil}}{\Delta x_i + \Delta x_{i+1}}$$

$$a_i^{J+1} = a_i^J \quad (44)$$

It should be noted that for all the above relations, the positive coefficient criterion must be satisfied[16].

The simulation procedure is based on the above mentioned relations. For a salt pan with given parameters, site and starting date, its transient behavior can be easily determined provided the time dependent meteorological conditions and solar radiation are known.

Meteorological conditions are adopted from actual measured data in our simulations, and time interval for all meteorological conditions in the simulation is 15-minute.

RESULTS AND DISCUSSION FACTORS AFFECTING THE BEHAVIOR OF THE SALT PAN

From equation (14) it seems that to intensify the process of evaporation, $\rho_{w,s}$ and thus the temperature of brine T_w should be raised, but when the temperature of brine goes up, the heat losses also increase. In order to illustrate the relation between the brine temperature and the evaporation rate (i.e., the evaporated water mass of a unit area in a minute) in the simulated days, the curves of various heat losses and the energy for the use of evaporation of brine with the brine temperature in salt pans are shown in Fig.2. In the simulations, the thermal properties of soil are taken as: $K_{soil} = 0.52$ W/m/K, $\rho_{soil} = 1840$ kg/m^3 and $C_{soil} = 2025$ J/kg/K. From Fig.2 we can see that the rate of evaporation with the brine temperature increases faster than that of heat losses. This means the evaporation process is greatly intensified when the temperature of brine increases.

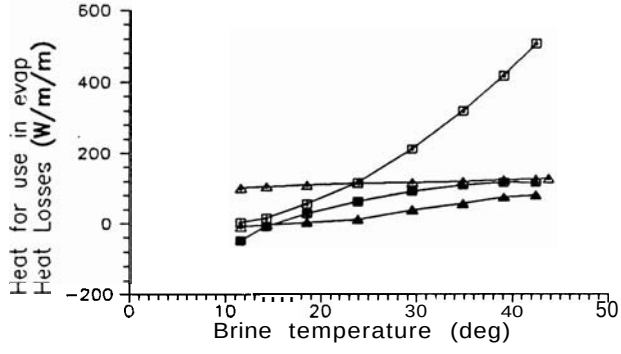

Fig.2 The effects of brine temperature on the heat losses and heat for the use of evaporation
□ heat for the use of evaporation
A radiation ● conduction
A convection

All the following simulations, unless particularly pointed out , are carried out with the depth of brine layer 0.02 m, and the absorptance of soil surface 0.92, depth of water table 8 m.

The Effect of the Depth of Brine Layer

One way to increase the temperature of brine is to reduce the heat capacity of the brine layer, in other words, the depth of the brine layer. Figs.3 and 4 show the typical time dependent profile of the solar radiation, the evaporation rate and the brine temperature under typical salt pan parameters and meteorological conditions in May in a Jiangsu saltern, China. As seen from Fig.3, for a salt pan with a thin brine layer (0.02 m), the profile of evaporation rate of brine is almost the same as that of the insolation except for a short

time lag, the brine reaches its maximum temperature near noon (13:30) when the sunshine is most intensive, the ambient temperature highest and the relative humidity lowest, then the temperature of brine falls, and drops to its lowest point (about 5 °C lower than the ambient temperature) at about 5:00 A.M. When the ambient temperature is lowest and relative humidity highest in the simulated days, in the meantime, a negative evaporation (water condenses onto the surface of brine layer) occurs. But when the brine layer is 0.4 m thick, the temperature profile of the brine is quite different from that shown in Fig.3, i.e. the temperature of brine increases slowly and almost continuously in

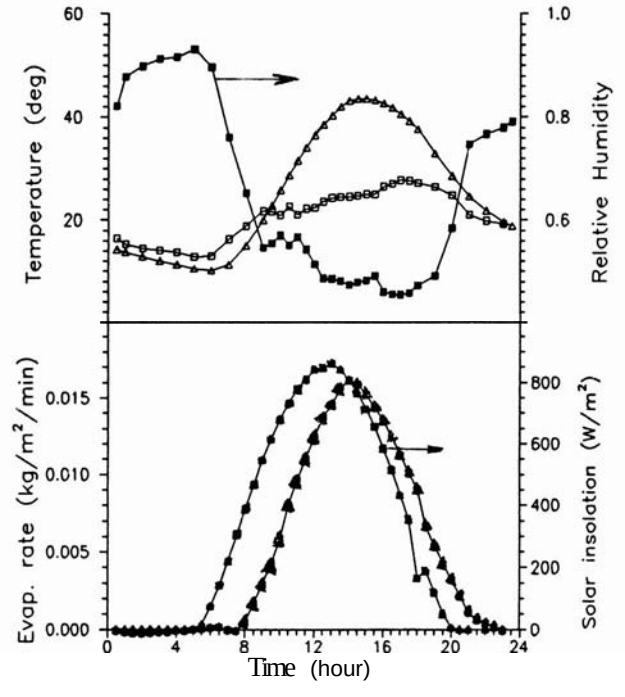

Fig.3 The transient behavior of the salt pan with the depth of brine layer of 0.02 m
A brine temperature
□ ambient temperature
A evaporation rate
▮ solar insolation
● relative humidity

the daytime, decreases very little after sunset, and although the maximum brine temperature of the salt pan with deep brine layer is much lower than that of salt pan with thin brine layer, the lowest temperature of brine during the nighttime is much higher than that of salt pan with thin brine layer (see Fig.4). For the particular situations shown in Fig.3 and Fig.4, the temperature difference of maximum temperature reached during the daytime of the two salt pans is 16°C, while the difference of lowest temperatures of the two salt pans is 10°C. The profiles of the evaporation rate of brine are also quite different for the two salt pans; the evaporation rate of deep salt pan is lower during the daytime but higher after sunset compared to that of shallow salt pan.

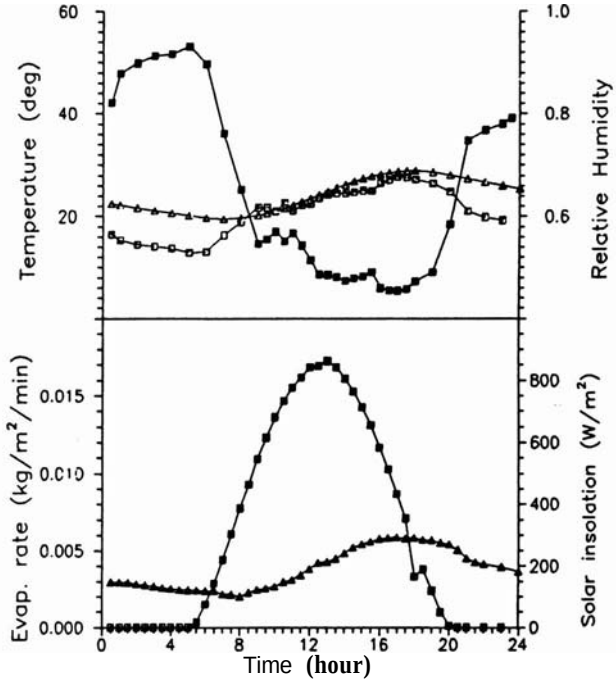

Fig.4 The transient behavior of the salt pan with the depth of brine layer of 0.4 m
A brine temperature
□ ambient temperature
A evaporation rate
▮ solar insolation
● relative humidity

Simulations show that:

(1). Approximately 95% of the evaporation occurs during daytime (7 a.m. to 7 p.m.) when the depth of the brine layer is 0.02 m, that means most of the incident solar radiation received by the salt pan in daytime is used for evaporation and little energy is stored. But for a salt pan with a deep brine layer (0.40 m), only 50–60% of the evaporation occurs during the day (7 a.m. to 7 p.m.). This is because the salt pan with a deep brine layer is able to store energy and shift the evaporative process to nighttime hours.

(2). The total evaporated mass of water from the salt pans with thin brine layer outpaces that with thick brine layer, especially in bad weather conditions. This can be easily explained as follows: a thin brine layer has a small thermal capacity and so has a small thermal storage and short response time for solar radiation, hence the brine is heated up faster, the evaporation rate increases more rapidly, the solar radiation absorbed by the brine and soil surface is used to evap-

orate brine almost synchronously. But for salt pans with deeper brine layer, most of the solar radiation absorbed is stored in the brine layer due to its large thermal storage capacity, and the temperature of brine maintains at a relatively higher level at night. During the night the ambient temperature is lower than in daytime, so heat losses to the surrounding environment by convection and radiation are greater than that of salt pan with a thin brine layer, and hence, more of the energy stored in the salt pan during daytime is likely to be lost through convective and radiative heat transfer rather than to produce evaporation. Besides, the relative humidity of the ambient air is higher at night, making the evaporation rate lower. In short, energy storage reduces evaporation rate of brine.

(3). Under bad weather conditions, salt pan with thin brine layer has important advantages compared with deep brine layer. This is because when the solar radiation is weak or intermittent, the brine temperature of salt pans with deept layer can only rise to a temperature a little higher than that of the ambient air, whereas the brine temperature of salt pans with thin layer increases quite significantly. For a particular meteorological conditions (shown in Fig.5), the maximum brine temperature can reach up to 40°C (13°C higher than the maximum ambient temperature in the simulated day) when the depth of brine layer is 0.02 m, while that of deep salt pan (0.2 m) can only reach 25°C. The total evaporated water mass for a single day is 3.50 kg and 2.92 kg respectively.

Effect of Absorptance of Soil Surface

Another way to intensify the evaporation process is to increase the absorptance of the soil surface of the salt pan. Fig.6 shows the effect of the absorptance of soil surface on the evaporated mass of water. As seen from the figure, the higher the absorptance of the soil surface, the larger the evaporated mass. Results also show that when the brine layer is thin (say 0.02 m), the absorptance of the soil surface plays a more important role on the evaporation rate than for deep brine layer. For a particular simulation, the evaporated mass of water dropped from 7.2 $kg/m^2/day$ to 5.3 $kg/m^2/day$ when the absorptance ot soil surface is reduced from 0.95 to 0.80. But when the brine layer is very deep, say 60 cm, the evaporated mass of water only dropped 16% when the absorptance of soil surface is reduced from 0.95 to 0.50. This is due to the fact, that for a salt pan with a very thin brine layer, the fraction of solar radiation absorbed by the brine layer is very small, and most part of solar radiation is absorbed by the soil surface. In contrast to this, when the brine layer is very deep, most of solar radiation is absorbed by the brine itself, and the fraction of solar radiation reaching the soil surface of the salt pan is small.

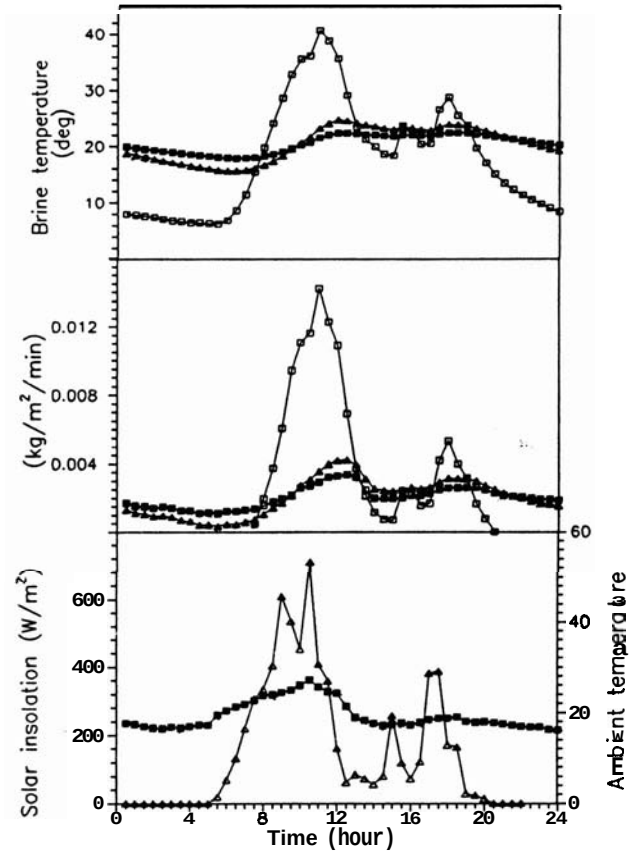

Fig.5 The effect of the brine layer depth on the evaporation rate on bad weather
□ D_w=0.02m A solar insolation
A D_w=0.2m ■ ambient temperature
● D_w=0.4m

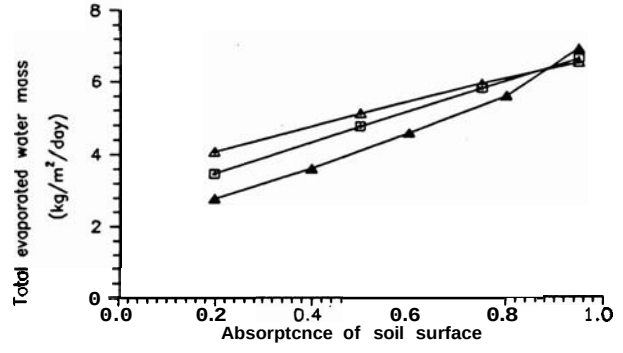

Fig.6 The effect of absorptance of soil surface on the evaporated water mass
A D_w=0.02m □ D_w=0.2m
A D_w=0.4m

It should be noted that the comparisons are carried out with the same initial temperature of brine and soil, and the terminal temperatures of the brine layer and soil for different absorptances of soil surface

on the simulated days are quite different. The larger the absorptance of tlie soil surface and the deeper the brine layer, the higher the ending brine temperature, which means the salt pan with higher absorptance of soil surface and deeper brine layer can store more energy than with lower absorptance of soil surface and shallow brine layer. Although the energy storage in the brine layer and soil reduces the evaporation rate of the day, it provides the salt pan with a higher initial temperature for the following day. Therefore, if long term performance is considered, the effect of absorptance of soil surface should be a little larger than shown in Fig.6.

Effect of Absorptance of Brine

Simulations are also performed by varying the absorptance of brine. Attempts have been made in some experimental salt pans in China to change the color of the brine layer so as to increase the absorptance of brine: some were added with dye or pigment to the brine layer, and in others algae or microbe with dark red color were bred in the brine layer. Unfortunately, all these attempts have their disadvantages. For example, when dye or pigment was added to the brine layer, the salt obtained inevitably carried the color of the added dye or pigment.

Results show that although the absorptance of brine plays a vital role in the process of evaporation as does the absorptance of soil surface, increasing the absorptance of brine is not as superior as anticipated to the increase of the absorptance of soil surface, especially for the salt pan with a thin brine layer. This can be rationalized by the idea that the thermal resistance of soil surface to the ground is much greater than that of the soil surface to brine, and hence most of the energy absorbed by the soil surface is transferred to the brine layer and is used for the evaporation of brine. However, for the salt pan with a deep brine layer, the effect of adding dye to the brine is expected to be more pronounced. This is because the assumption of uniform temperature in tlie brine layer is no longer valid in this case, a stratification of brine layer should be established[17], and a higher temperature and saturated vapor pressure at tlie brine surface are expected. Such a problem is more complicated, and does not seem to be of any significance in the salt pan simulations, and hence is omitted here. Computer simulations have been carried out for two salt pans on the condition that tlie absorptance of brine of one salt pan equals the absorptance of soil surface of another one. Results show that the difference of the evaporation rate of two salt pans is almost negligible. Therefore, in practical salt pans for making edible salt, increasing the absorptance of soil surface is recommended.

Effect of Thermal Conductivity of Soil and Extra Insulation Layer

Fig.7 shows the profiles of conductive heat loss from the soil surface to the ground with different thermal conductivities of soil. It is found that: (1) The conductive heat loss is positive in daytime and negative at night. In other words, the bottom of the brine layer transfers energy to the soil during daytime and extract energy from the soil at night; (2) Although the profiles of conductive heat loss are quite different, the evaporated water mass does not show much difference. This can be interpreted as follows: most of the energy transferred to the ground during daytime is stored in the soil itself to increase the ground temperature, and goes back to the brine at night when the ambient temperature and brine temperature are lower, and the more is the energy transferred to the ground in daytime, the larger will be the quantity of energy recovered at night.

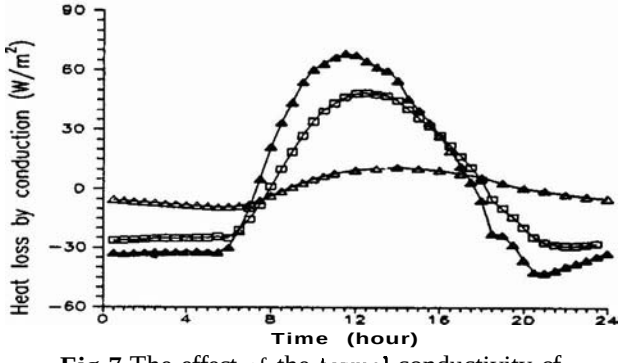

Fig.7 The effect of the termal conductivity of soil on conductive heat loss
A k_{soil}=1.4 W/m/K
A k_{soil} 0.026 W/m/K
□ k_{soil}=0.52 W/m/K

In some experimental salt pans in China, a thin layer of insulation material is added over the soil surface of tlie salt pan in order to reduce conductive heat loss and to prevent the leakage of brine to the soil, and thus to increase the production of salt. As a special example, a 10 cm air insulation layer was simulated to illustrate the effect of the insulation layer.

Calculations show that the evaporated water mass of a salt pan with a 10 cm air insulation layer only differs by 6%–8% from that without any insulation when the salt pan is built on dry clay (k_{soil} = 1.2 W/m/K) with tlie depth of water table greater than 8 meters, and 8%–10% from the salt pan built on wet soil (k_{soil} = 2.2 W/m/K) with the depth of underground water table D_g = 5 m. This is also due to the high thermal resistance of the ground and the low thermal resistance of brine to air.

From the above mentioned results it seems that when the salt pan is built on dry clay with a deep underground water table, it may not be so cost effective to insulate it.

Effect of Depth of Water Table and Weather Conditions

Simulation results show that the effect of the depth of water table on the evaporated water mass during a 24–hour period is almost negligible when the depth of water table is greater than 5 meters. This result also conforms to the analytical solution of an infinite plane with a sinusoidal temperature variation on the surface set out by Liakatas et al[18], that is, at a depth given by

$$d_s = 1.6(\pi\alpha\Delta\tau)^{0.5}$$

only 1% of the top ground temperature variation is detected after a given time interval AT.

Meteorological conditions, such as the wind speed, relative humidity, ambient temperature, of course, also have important effects on the behavior of the salt pan. But the mefeorological conditions are not at our disposal, and hence are neglected herein. But some basic relations between the evaporation rate and meteorological conditions can be easily derived from formulae listed in section 2 of this paper: an increase in the wind speed and the ambient temperature and a decrease in the ambient relative humidity will cause an increase in the evaporation rate of brine.

CONCLUSIONS

The proposed simulation model provides very valuable information about the importance of each factor or parameter involved in the general behavior of the salt pan. This information can assist the designer and operating worker of the salt pan to select proper construction and optimum configuration for maximum utilization of available solar radiation.

It is found that the depth of the brine layer plays a very important role on the evaporation rate of brine on bad weathers, although it is not so important in fine weathers. The absorptance of soil surface, the absorptance of brine layer and the insolation also have important influence on the evaporative process to make salt.

In practical saltern, the moisture content of the soil is usually very high, and its thermal conductivity is also very high and, therefore, if the cost of insulation is economically acceptable, insulating the salt pan is recommended.

Acknowledgements

This research project was funded by a grant from the National General Salt Company of China. We are Grateful to Prof. S.X. Cheng (USTC) for his valuable comments.

REFERENCES

[1] H. Tabor, "Large Area Solar Collectors (Solar Pond) for Power Production," Proceedings of the UN Conference on the New Sources of Energy 4, p.59, (1964).

[2] H. Tabor, and R. Matz, "Solar Pond Project," *Solar Energy, 9*, p.177, (1965).

[3] J.R. Hull, "Membrane Stratified Solar Pond," *Solar Energy,* 24, p.317, (1980).

[4] E.S. Wilkins and T.K. Lee, "Development of the Gel Pond Technology," *Solar Energy,* 31, p.33, (1987).

[5] U. Ortabasi, F.H. Dyksterhuis and W.D. Kaushika, "Honeycomb Stabilized Saltless Pond," *Solar Energy,* 27, pp.229–231, (1983).

[6] G.R. Guinn and B.R. Hall, "Solar Production of Industrial Process Hot Water Using Shallow Solar Pond," Proceedings of the Solar Industrial Process Heat Symposium, pp.161, (1977).

[7] M. Sokolov and A. Arbel, "Freshwater Floating–Collector–Type Solar Pond," *Solar Energy,* 34, No.1, pp.13–21, (1990).

[8] W.D. Lu and H.F. Guo, "A Preliminary Research on the Latent Solar Pond," *Acta Energiae Solaris Sinica,* 13, No.1, (1992), (in Chinese).

[9] K. Kanayama and H. Baba, "Transmittance of Distilled Water and Sodium–Chloride–Water Solutions," *Journal of Solar Energy Engineering,* 110, p.113, (1988).

[10] X.M. Ye, A.G. Song and G.S. Lee, "Refractive Index of Salt Solutions in Solar Pond," *Acta Energiae Solaris Sinica,* 8, No.1, (1987), (in Chinese).

[11] J.A. Duffie and W.A. Beckman, ≪Solar Energy Thermal Processing>>, Joha Wiley & Sons, (1974).

[12] X.S. Ge, B. Gong, W.D. Lu and Y.F. Wang, ≪Solar Energy Engineering≫, Academic Periodical Press, Beijing, (1988), (in Chinese).

[13] F.P. Incropera and D.P. Dewitt, ≪Fundamentals of Heat Transfer≫, John Wiley & Sons, (1981).

[14] S. Globe and D. Dropkin, "Natural Convection Heat Transfer in Liquids Confined between Two Horizontal Plates," *J. Heat Transfer,* 81 C, 24, (1959).

[15] S.Y. Liu and Y.F. Huang, "The Effective Sky Temperature? *Acta Solaris Energiae Sinica,* 4, No.1, pp.63–68, (1988), (in Chinese).

[16] S.V. Partankar, <<Numerical Heat Transfer and Fluid Flow>>,McGraw–Hill New York, (1980).

[17] M.S. Sohda, A. Kumar, G.N. Tinari and G.C. Pandey, *Appl. Energy, 7*, pp.147–162, (1980).

[18] A. Liakatas, J.A. Clark and J.L. Monteith, "Measurement%of Heat Balance under Plastic Mulches," *Agricultural and Forest Meteorology* 36, pp.227–239, (1986).